Folia Microbiol (2016) 61:283–293
DOI 10.1007/s12223-015-0436-5

Synthesis of silver nanoparticles on the basis of low and high molar mass exopolysaccharides of *Bradyrhizobium japonicum* 36 and its antimicrobial activity against some pathogens

Bakhtiyor Rasulov[1,2] · Nigora Rustamova[2,3] · Abulimiti Yili[2] · Hai-Qing Zhao[2] · Haji A. Aisa[2]

Received: 1 September 2015 / Accepted: 18 November 2015 / Published online: 24 November 2015

Abstract Silver nanoparticles (SNPs) were synthesized on the basis of exopolysaccharides (low and high molar mass) of diazotrophic *Bradyrhizobium japonicum* 36 strain. The synthesis of SNPs was carried out by direct reduction of silver nitrate with ethanol-insoluble (high molar mass, HMW) and ethanol-soluble (low molar mass, LMW) fractions of exopolysaccharides (EPS), produced by diazotrophic strain *B. japonicum* 36. SNPs were characterized using UV-vis spectroscopy, transmission electron microscopy (TEM), X-ray diffraction (XRD), and Fourier transform infrared spectroscopy (FTIR). SNPs synthesized on the basis of LMW EPS absorbed radiation in the visible regions of 420 nm, whereas SNPs based on the HMW EPS have a wavelength maximum at 450 nm because of the strong SPR transition. Moreover, the antibacterial and antifungal activities of the SNPs were examined in vitro against *Escherichia coli*, *Staphylococcus aureus*, and *Candida albicans*. SNPs synthesized on the basis of LMW EPS were active than those synthesized on the basis of HMW EPS. Besides, UV-visible spectroscopic evaluation confirmed that SNPs synthesized on the basis of LMW EPS were far more stable than those obtained on the basis of HMW EPS.

✉ Haji A. Aisa
haji@ms.xjb.ac.cn

[1] Institute of Genetics and Plant Experimental Biology, Uzbekistan Academy of Sciences, Kibray District, Yukori Yuz, 111126 Tashkent, Uzbekistan

[2] Key Laboratory of Plant Resources and Chemistry in Arid Regions, Xinjiang Technical Institute of Physics and Chemistry, Chinese Academy of Sciences, South Beijing Road 40-1, Urumqi, Xinjiang 830011, People's Republic of China

[3] Department of Biology, Samarkand State University, University Boulevard 15, Samarkand 703004, Uzbekistan

Introduction

Recent advances in nanotechnology have enabled us to produce pure silver as nanoparticles, which are more efficient than silver ions (Lara et al. 2010), and because of their surface plasmon resonance properties, silver nanoparticles (SNPs) have become the focus of extensive research due to their wide range of applications, such as in medicine, agriculture, catalysis (Hebeish et al. 2013), colorimetric sensors, optical encoding, and metal-enhanced fluorescence (Shafer-Peltier et al. 2003; De Cremer et al. 2010; Aslan et al. 2005). Conventionally, SNPs are synthesized using chemical reducing agents in the presence of stabilizers (Kanmani and Lim 2013a, b). Except chemical methods, some green methods have been documented for the biosynthesis of SNPs. Some bacteria (*Lactobacillus rhamnosus* (Kanmani and Lim 2013a), *Bacillus licheniformis*, *Staphylococcus aureus* (Kalimuthu et al. 2008; Nanda and Saravanan 2009), and fungi (*Alternaria alternata*, *Aspergillus flavus*, *Penicillium* (Gajbhiye et al. 2009; Jain et al. 2011) have been successfully studied for the biosynthesis of SNPs. Furthermore, SNPs have received the greatest attention due to their wide spectrum of antimicrobial activities towards many Gram-positive and Gram-negative bacteria, fungi, and viruses (Lara et al. 2010; Hebeish et al. 2013; Shafer-Peltier et al. 2003). Microbe-based biosynthesis of SNPs has several advantages such as simplicity, cost effectiveness, and compatibility for biomedical and pharmaceutical applications as well as for large-scale commercial production (Filippo et al. 2010). This has opened up whole new strategies to use pure silver against a wide range of

pathogens, particularly multiresistant pathogens, which are hard to treat with available antibiotics. One of the microbial reducing and stabilizing agents are exopolysaccharides and they are increasingly being used to synthesize silver nanoparticles. These macromolecular biopolymers contain many hydroxyl groups that strongly associate with metal ions leading to greater control of shape, size, and particle dispersion. Moreover, polysaccharides have other valuable functions such as mucoadhesion, which provides a greater neutral coating with low surface energy and restricts nonspecific protein receptor recognition (Santander-Ortega et al. 2012). Exopolysaccharides (EPS) are long-chain polysaccharides containing branched and repeating units of sugar molecules, such as glucose, mannose, fructose, or rhamnose (Kanmani et al. 2012). These natural biopolymers have been widely used as viscosifying, bioflocculating, stabilizing, gelling, and emulsifying agents. The lack of microbe-based synthesis of SNPs is due to low solubility of bacterial polysaccharides and instability of produced SNPs, once silver ions were reduced and stabilized on a bacterial EPS matrix. To our knowledge, this can be explained by long molecular chain of bacterial EPS and due to the collision between small nanoparticles, which lead to particle growth (Dang et al. 2011). All data documented in the literature on synthesis of SNPs was obtained by relatively high molar mass EPS of bacteria, but there is no report on using low molar mass EPS for SNPs synthesis, despite the fact that synthesis of low molar mass EPS occurs along with synthesis of high molar mass EPS in cells of some bacterial species. Low molar mass forms of EPS have previously been identified in *Sinorhizobium meliloti* cultures (Battisti et al. 1992), and ethanol-soluble low molar mass EPS in *Bradyrhizobium japonicum* been reported by Louch and Miller (2001). Recently, studies of SNPs synthesis through silver reduction and stabilization on water-insoluble EPS, with high molar mass, of *B. japonicum* 36 strain was reported (Rasulov 2014), but SNPs synthesis using low molar mass EPS was not still researched.

In this study, we studied the synthesis of silver nanoparticles by direct reduction of silver nitrate with ethanol-insoluble (high molar mass) and ethanol-soluble (low molar mass) EPS, produced by diazotrophic strain *B. japonicum* 36. The synthesized SNPs were characterized using UV-vis spectroscopy, transmission electron microscopy (TEM), X-ray diffraction (XRD), and Fourier transform infrared spectroscopy (FTIR). Moreover, the antibacterial and antifungal activities of the SNPs were examined in vitro. Throughout the research, high molar mass (HMW) EPS and SNPs synthesized on its basis were used for comparative study to estimate SNPs, synthesized on the basis of low molar mass (LMW) EPS.

Materials and methods

Materials and microbial strains

The exopolysaccharide-producing diazotrophic strain *B. japonicum* 36 (strain's collection number SDK 276), deposited at the Culture Collection of Industrial Microorganisms (860, CCIM) at the Institute of Microbiology, Uzbekistan Academy of Sciences, was used. The pathogenic strains *Candida albicans* ATCC10231, *Escherichia coli* ATCC11229, and *S. aureus* ATCC6538 were obtained from the Culture Collection of State Key Laboratory Basis of Xinjiang Indigenous Medicinal Plants Resource Utilization, Xinjiang Technical Institute of Physics and Chemistry, CAS.

All solutions were made of using ultrafiltered high-purity deionized water. Reagents and chemicals used in this study were of analytical grade.

Extraction of EPS from B. japonicum 36

EPS-producing *B. japonicum* 36 was cultured in a 2 L conical flask containing 1 L of "79" broth at 30 °C. After 3 days incubation, the cultured broth was heated to 100 °C for 15 min to inactivate the EPS-degrading enzymes. Subsequently, the treated culture broth was centrifuged at 6000 rpm for 10 min at 4 °C to separate the probiotic cells and debris. The cell-free supernatant was collected and mixed with a double volume of ice-cold ethanol (95 %) and maintained at 4 °C overnight to complete the precipitation of EPS. After centrifugation at 12,000 rpm for 15 min, the precipitated EPS pellet was washed twice with distilled water and recovered by adding 20 mL of water (Rasulov et al. 2013). The concentration of EPS in the solution was quantified by the phenol-sulfuric acid method (Dubois et al. 1956).

Fractionation and analysis of low molar mass exopolysaccharide from B. japonicum 36 culture and thin-layer chromatography

B. japonicum 36 strain was cultured in 500 mL of 79 medium at 30 °C until reaching an optical density of 0.6 at 650 nm. The cells were harvested (13,000 g for 10 min), and culture supernatants were obtained. The culture supernatants were concentrated 25-fold by rotary evaporation. High molar mass EPS were precipitated from concentrated supernatants by adding three volumes of ice-cold ethanol, and the precipitate was removed from concentrated supernatants by centrifugation at 12,000 g for 10 min. Low molar mass ethanol-soluble polysaccharide was then purified from concentrated supernatants using gel permeation chromatography as described below.

Concentrated supernatants containing ethanol-soluble, extracellular low molar mass polysaccharide was concentrated under vacuum. Samples were applied to a Sephadex G-25

column (1 cm×52 cm) which was eluted at room temperature with 0.15 mol/L ammonium acetate (pH 7.0) containing 7 % propanol (vol/vol) at the rate of 15 mL/h. Fractions (1 mL) were collected and assayed for carbohydrate content (Dubois et al. 1956). Thin-layer chromatography (TLC) was performed using aluminum-backed silica gel 60 plates and a butanol-ethanol-water (5:5:4) solvent system.

Synthesis of SNPs using EPS

The solution of EPS (100 mL) was mixed with 10 mol/L aqueous solution of $AgNO_3$ prepared freshly in deionized water with continuous stirring. The mixture was stored at room temperature for 2 months. After 24 h incubation, the solution turned yellow and after a while dark brown, which confirmed the formation of SNPs (Kanmani and Lim 2013a).

Characterization of silver nanoparticles

UV-visible spectroscopy analysis

EPS reduction of Ag^+ ions in aqueous solution was monitored for 12 h, 5 days, 10 days, and 2 months by measuring the ultraviolet–visible absorbance spectrum of the solution using a UV-visible spectrophotometer (TU-1901, Beijing Purkinje General Instrument Co., Ltd.) in the range of 300–800 nm (Kanmani and Lim 2013a).

Transmission electron microscopy

TEM micrographs were obtained on a HITACHI H-600 transmission electron microscope (Hitachi, Japan) operating at an accelerating voltage of 100 kV (Kanmani and Lim 2013a).

Analysis of the XRD and FTIR spectra

The phase composition and crystal structure of the SNPs was determined using XRD (Bruker D8 Advance). For this analysis, the dried sample was prepared by placing on the microscopic glass slide and the diffractogram was recorded using Cu-Kα radiation and a nickel monochromator filtering wave at voltage and current of 40 kV and 30 mA, respectively. The FTIR spectrum of the EPS-stabilized SNPs was analyzed using FTIR spectroscopy (JASCO FTIR 460, Daejon, South Korea) operated at resolution of 4/cm. For the measurement of FTIR spectrum, the dried sample was powdered by grinding with KBr pellets and pressed into a mold. The spectrum was recorded at a frequency range of 500–4000/cm (Li et al. 2012).

Antibacterial and antifungal activities of SNPs

Incubation of pathogenic strains

All bacterial strains were cultured following manufacturers' culturing guidelines. Typically, *E. coli* ATCC11229 and *S. aureus* ATCC6538 strains were cultured in Luria-Bertani (LB) culture medium (10 g/L tryptone, 5 g/L yeast extract, 10 g/L NaCl) at 37 °C. In all the experiments, the concentrations of bacteria were determined by optical density at 600 nm.

C. albicans ATCC10231 was cultured in culture medium comprising glucose 40 g/L and peptone 10 g/L (Bankura et al. 2012).

The agar well diffusion method

The antibacterial and antifungal activities of the EPS-stabilized SNPs were measured using the agar well diffusion method. Bacterial and fungal pathogens such as *E. coli*, *S. aureus*, and *C. albicans* were used as indicator strains for this analysis. The bacterial and fungal strains were aseptically inoculated into respective broth and then incubated at 37 °C. Samples from the culture liquids of respective pathogen plated on petri plates and wells were made using an agar well borer. Different concentrations of SNPs were added to these wells, and the plates were incubated at 37 °C for 24 h. The zone of inhibitions was estimated by measuring the diameter of the bacterial growth inhibition zone. The values were averaged from the three independent experiments (Bankura et al. 2012).

Kill-curve experiments (I)

The overnight bacterial cultures were diluted in fresh LB media, supplemented in different concentrations of SNPs both in colloidal and powder forms and incubated at 37 °C for 1 week. The culture liquids were analyzed for cell number by counting colony forming units on each incubation day (Kim et al. 2011).

Kill-curve experiments (II)

SNPs were added in different concentrations, in a powder (μg/mL) and colloidal (mL) forms, to the two days old bacterial cultures (CFU not less than 10^9 cells per mL), and incubated at 37 °C for next days. From the third day of incubation (the day after SNPs addition), the cell number of the strains was evaluated via plating corresponding serial dilutions of the bacterial cultures. Estimations continued until seventh day of incubation (Kim et al. 2011).

Results

UV-vis spectrophotometer

The synthesis of SNPs in the solution was monitored by UV-visible absorption spectra. As it was mentioned before, SNPs were synthesized by reducing Ag^+ to Ag^0 with addition of LMW and HMW EPS in a solution of $AgNO_3$ and then the samples were left in the dark. In order to obtain the maximum productivity of SNPs by EPS, different ratios of reducer and the silver nitrate (1:1, 2:1) were assessed. Visually, synthesis of SNPs was estimated by formation of yellowish brown color in colorless solution. In our experiments, SNPs were synthesized on the basis of LMW EPS absorbed radiation in the visible regions of 420 nm, whereas SNPs on the basis of HMW EPS—450 nm because of the strong surface plasmon resonance (SPR) transition (Fig. 1a). The appearance of the SPR transition in this region confirmed the production of SNPs (Bankura et al. 2012; Pandey et al. 2012). Further evaluation of concentration dependence showed that with increasing both EPS (in our experiments, LMW) and silver nitrate concentrations, the formation of SNPs enhances (Fig. 1b). The increasing the concentration of silver nitrate added to the EPS solution resulted in a substantial increase in the SPR bands and reached its maximum when 10 mol/L silver ions were used.

Morphological and structural characterization of EPS-stabilized SNPs

The morphological properties of EPS-stabilized SNPs, i.e., the size and shape, were analyzed with help of TEM. The TEM images of SNPs are presented in Fig. 2. As TEM observations revealed, the SNPs varied in size and shape, despite constant reaction conditions and initial concentrations of the substrates (both LMW and HMW EPS). As in Fig. 2, the SNPs are rod- and oval-shaped structures, with an average diameter of 5–50 nm. This may be explained by the collision between small nanoparticles, which leads to particle growth (Dang et al. 2011). In both cases, the LMW and HMW EPS matrixes synthesized absolutely identical SNPs in shape and size. This evidence may be explained with a number of repeating monomers in LMW and HMW EPS of *B. japonicum* species. Here we concluded that not the overall chemical structure of bacterial EPS takes part in reducing the silver ions and stabilizing them, but certain monomers of hydrocarbon nature play a crucial role in the formation of nanoparticles.

The higher concentration of initial compounds' molecules also resulted into potential agglomeration of many small nanoparticles. The obtained results are in agreement with those by other researchers.

Analysis of the XRD and FTIR spectra

XRD analysis provided significant information on the structure of SNPs, obtained on the matrixes of LMW and HMW EPS. In both cases, XRD spectra of the SNPs exhibited four peaks (Fig. 3a, b), which confirmed the presence of elemental silver in nanoscale. Out of the four peaks, three at 47.5, 55.5, and 64.5 were intensive in the 2 theta region. As it was documented by Pandey et al. (2012), these typical peaks occur due to the presence of a face-centered cubic (FCC) structure of SNPs.

FTIR estimation was carried out to investigate the possible functional groups and chemical bonds of EPS-reduced and EPS-stabilized SNPs. The FTIR spectra of SNPs, obtained by reducing and stabilization on the EPS of *B. japonicum* 36, exhibited various characteristic peaks with ranges from 3420 to 800/cm (Fig. 4). The broadest and strongest peak was observed at 3420/cm due to a stretching vibration of hydroxyl groups (O–H). The broad peaks at 1236–1063/cm correspond to C–O–C and C–O stretching, whereas the intense peak at 995/cm confirms the presence of carbohydrates. Furthermore, the weak absorption peaks at 820–972/cm were observed, which confirmed the linkages that had occurred between monosaccharides. The small peak at 1387/cm might be due to the influence of SNPs.

Antimicrobial activity

The agar well diffusion method

The antibacterial and antifungal activities of SNPs, synthesized by reducing Ag^+ ions with bacterial EPS, were investigated against the pathogen bacterial strains *E. coli* ATCC11229, *S. aureus* ATCC6538, and pathogenic fungi *C. albicans* ATCC10231 using the agar well diffusion method and via measuring the radial diameter of inhibition zones. The results revealed that all pathogens were inhibited after treatment with SNPs and the inhibition rate was proportionally depended on concentration (dilution) of SNPs. The radial diameters of inhibition zones are shown in Fig. 5. In high doses of SNPs, there were observed high inhibition zones, which could be due to the amount of silver ions, released from the SNPs–the reservoirs for silver ions (Feng et al. 2000).

Some researchers have documented antifungal activities of SNPs. Panacek et al. (2009) and Kanmani and Lim (2013a) reported growth inhibition of fungi *Candida*, *Aspergillus*, and *Penicillium* genera. A similar result was obtained by Panacek et al. (2009), who studied the antifungal activity of SDS-stabilized SNPs against various pathogenic strains of *Candida*. All strains were inhibited after treatment with SNPs. In our researches, the pathogenic strain *C. albicans* ATCC10231 inhibited by SNPs applied and formed 8-mm clear zone.

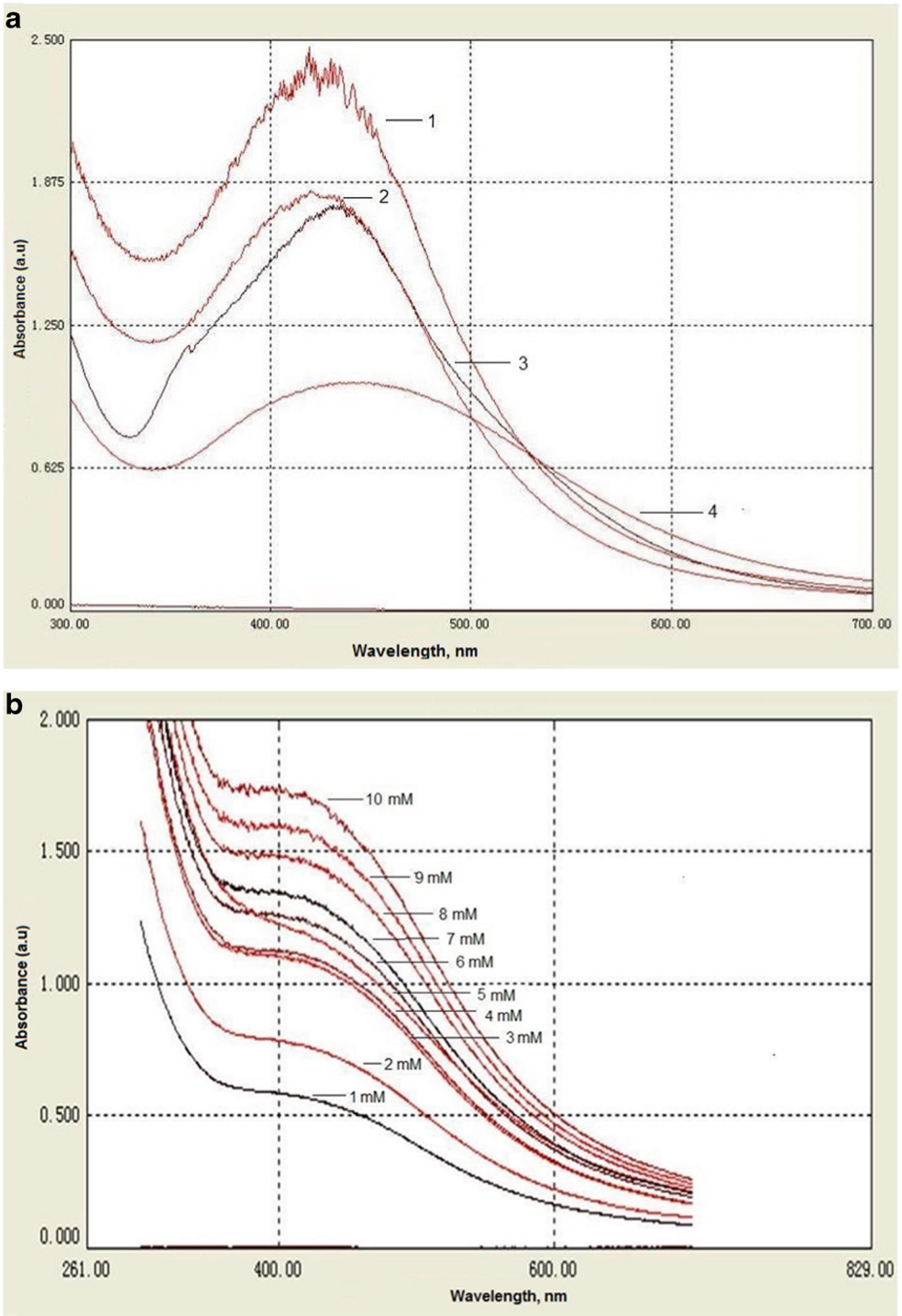

Fig. 1 **a** UV-vis spectra of SNPs, synthesized with EPS of *Bradyrhizobium japonicum* 36 (curves 1, 2–SNPs, synthesized on the matrix of LMW EPS; curves 3, 4–SNPs, synthesized on the matrix of HMW EPS; curves 1, 3–EPS and $AgNO_3$ in 1:1 ratio; curves 2, 4–EPS and $AgNO_3$ in 1:2 ratio). **b** UV-vis spectra of peaks produced by silver nanoparticles at different concentrations of EPS and silver nitrate at room temperature

Kill-curve experiments (I)

The antibacterial activity of SNPs was studied also in liquid medium; low (0.25–2.5 μg/mL) and high (up to 50 μg/mL) concentrations of SNPs, synthesized on the matrixes of LMW and HMW EPS, were evaluated against *E. coli* and *S. aureus* (Fig. 6). The pathogens were incubated in liquid medium, and their relative cell viabilities were estimated in different time intervals, i.e., for low concentrations of SNPs–up to third day incubation, whereas for high concentrations–within 12 h. In all the experiments, SNPs synthesized on the matrix of LMW EPS was far more active than that of HMW EPS. Treated with SNPs synthesized on the matrix of LMW EPS, it was observed that the relative cell viabilities were sharply reducing in early hours, and the remaining live cells after 12 h were at about 1.2×10^4–1.5×10^5 CFU/mL (Figs. 7 and 8). *S. aureus*

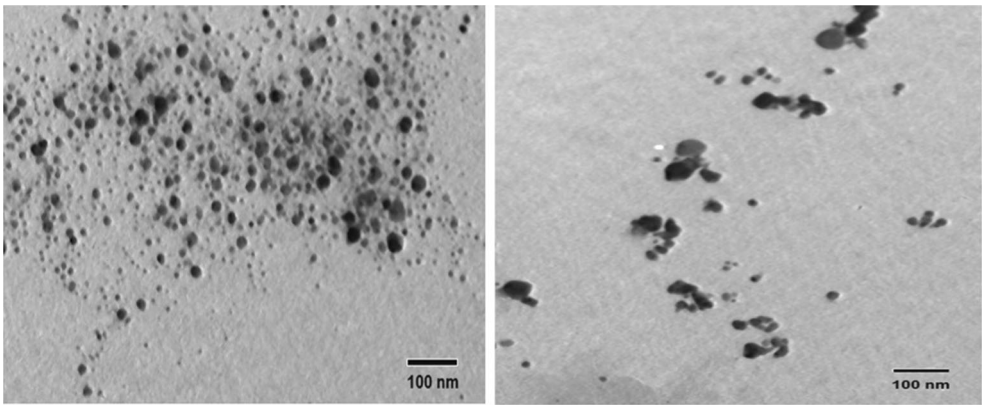

Fig. 2 TEM micrographs of EPS-reduced SNPs at different magnifications

ATCC 6538 was considerably sensitive than *E. coli* ATCC11229, and the pathogens failed to support normal growth in all tested concentrations. In 2.0 and 2.5 μg/mL concentrations of SNPs, 70–75 % of the cells of *S. aureus* ATCC 6538 were dead after 12 h incubation (Fig. 8). After the second and third days of incubation, all cell biomass were dead and precipitated into the bottom of the test tubes.

To obtain high efficiency of SNPs against the tested pathogens within a short period of time (from 0 to 12 h), high concentrations of SNPs (>2.5 μg/mL) were evaluated in the

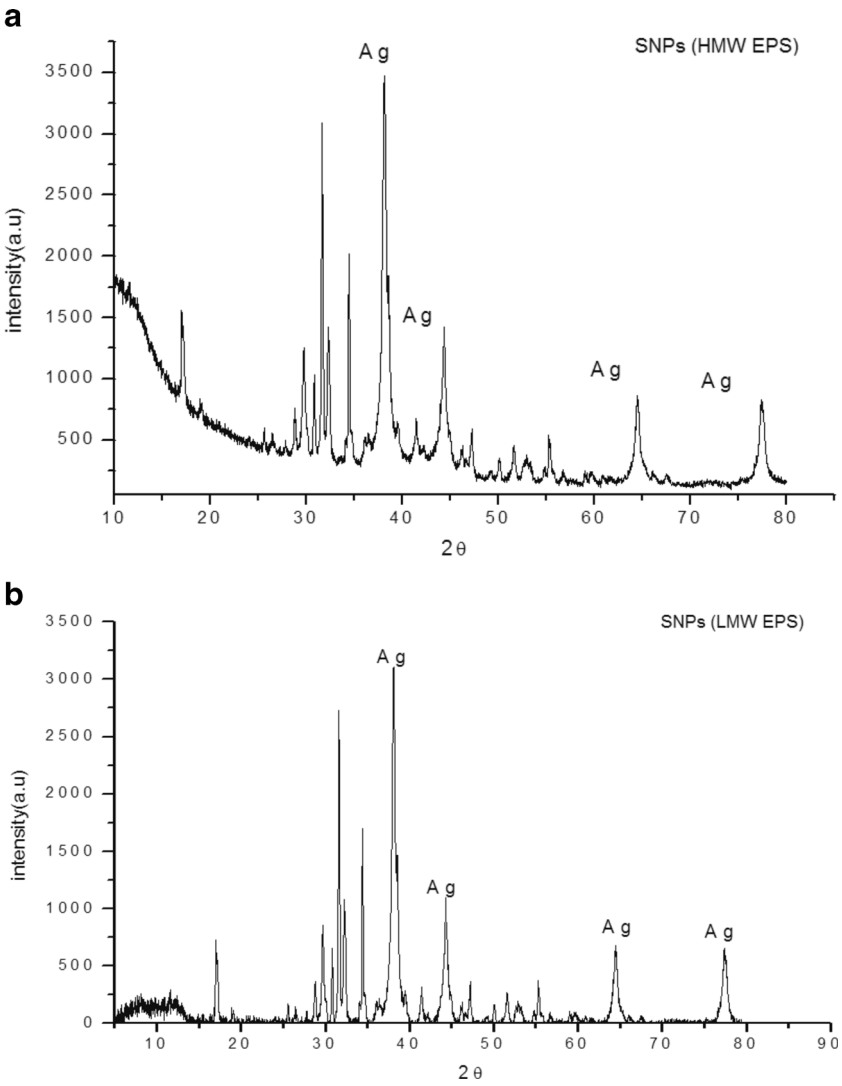

Fig. 3 **a** X-ray diffraction pattern the SNPs, synthesized on the matrix of HMW EPS. **b** X-ray diffraction pattern the SNPs, synthesized on the matrix of LMW EPS

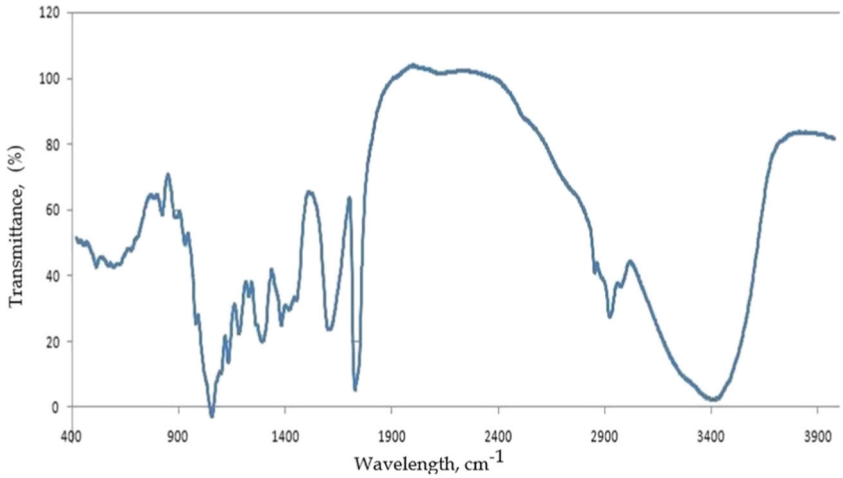

Fig. 4 FTIR spectrum of SNPs

other set of experiments. A wide range of SNPs concentrations were estimated, from 5 to 50 μg/mL; and in hourly basis, the relative cell viability was calculated. Increasing the SNPs' concentration resulted in shortening the time of SNPs' efficiency against the pathogens. After treatment with high concentrations of SNPs, the relative cell viability began to drop after 2 h of incubation.

Discussion

Since UV-visible absorption is a proven technique to analyze SNPs (Sastry et al. 1997), their formation can be confirmed by visual observation and measuring the surface plasmon resonance (SPR) band using UV-visible spectroscopy. The collective oscillations of conduction electrons at the surface of

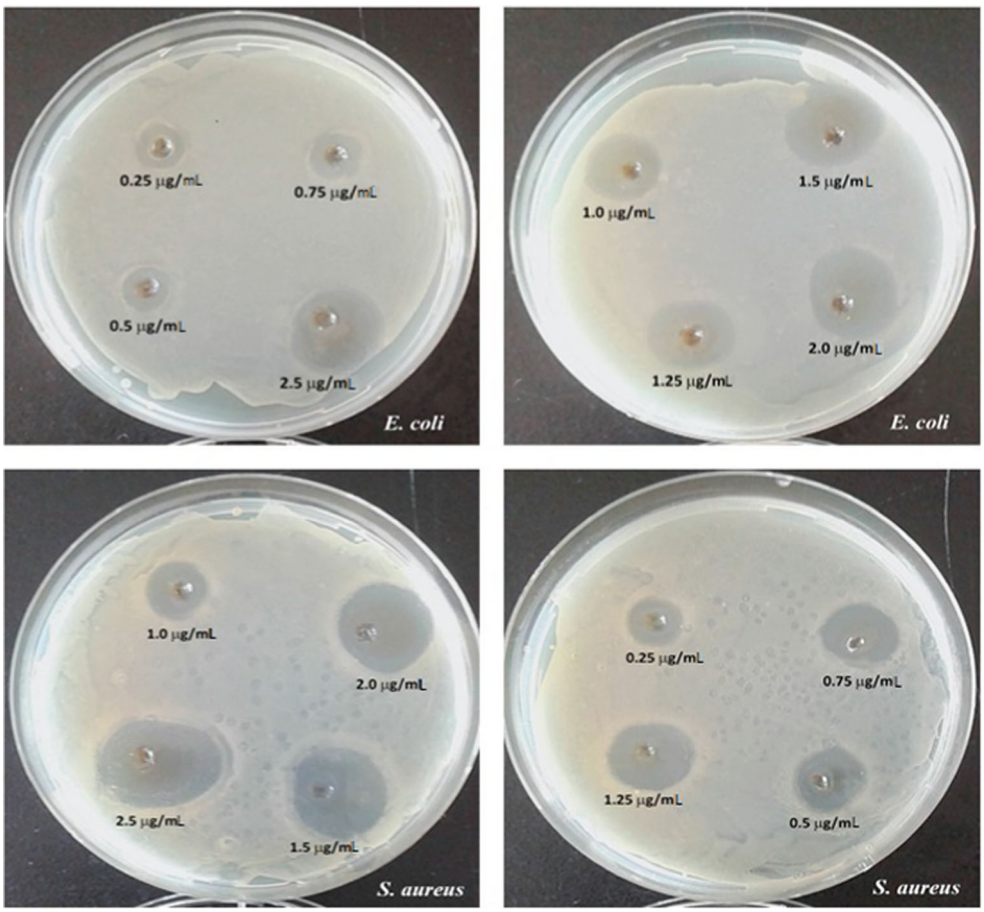

Fig. 5 Dose-dependent inhibition of the strains' growth by SNPs

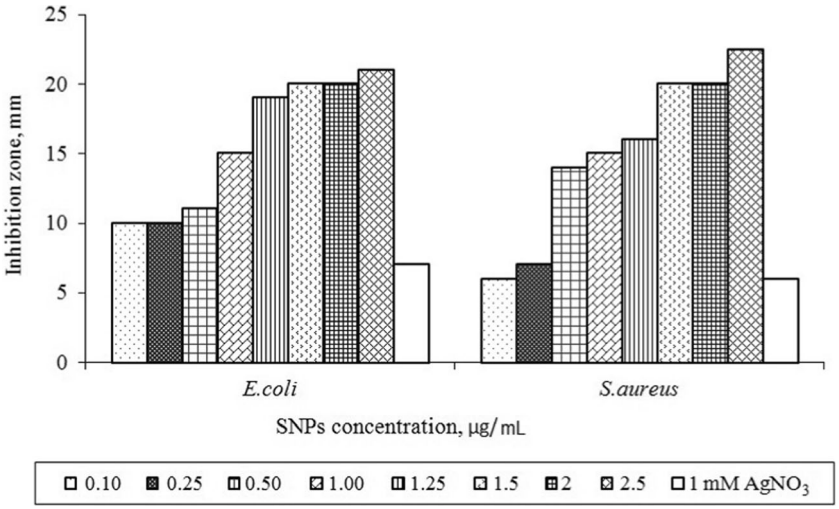

Fig. 6 Average diameter of inhibition zones of bacterial strains

nanosized metal particles absorb visible electromagnetic waves; the phenomenon is known as SPR (Dang et al. 2011). The SNPs usually reveal unique and tunable optical properties due to their strong SPR transition (Hebeish et al. 2013). Moreover, it is important to note that the synthesis and stability of SNPs in various methods depend on the concentration of the reducers (in our case, the EPS), Ag^{+} ions in solution, and incubation period of the reaction mixture (Hamedi et al. 2012; Kanmani and Lim 2013a). It is worth mentioning that the SPR of metal nanoparticles is greatly a size-dependent phenomenon. The electron-scattering enhancement at the surfaces of nanoparticles increases bandwidth and decreases the particle size. Hence, variations in bandwidth and shifts in resonance are very important parameters in characterizing the nanosized regime metal particles (Dang et al. 2011).

Colloidal SNPs are known to exhibit UV-visible absorption maximum in the range of 390–420 nm (Vigneshwaran et al. 2006). But EPS-stabilized SNPs showed strong SPR peak at 400–550 nm with a broad band due to the shape and size of colloidal SNPs (Kanmani and Lim 2013a, b). These two cases (absorption maximums) were observed in our experiments, when SNPs was synthesized on the matrixes of LMW and HMW EPS (Fig. 1a; curves 1, 2, 3, and 4). It helped to conclude that overall EPS (both LMW and HMW) of *B. japonicum* 36 can form two types of SNPs with absorption maximum at 420 nm (Fig. 1; curves 1 and 2) and absorption maximum at 450 nm (Fig. 1a; curves 3 and 4). Obtained data helped to make conclusion that LMW and HMW EPS of *B. japonicum* 36 and $AgNO_3$ form SNPs, which at the same time differ due to morphology, size, and stability. An analogical data was documented in the literature (Kanmani and Lim 2013a). This evidence might be due to the chemical structures of EPS of *B. japonicum*. As it was documented by Louch and Miller (2001) that *B. japonicum* also synthesizes a low molar mass-form extracellular EPS, along with high molar mass-form EPS (Quelas et al. 2006), which are different according to the physical and chemical properties.

Besides, it is clear that the EPS concentration is playing an important role in the reduction and stabilization of SNPs. The similar results were reported by Bankura et al. (2012) and Kanmani and Lim (2013b), who researched dose-dependent synthesis and stabilization of SNPs. Kanmani and Lim

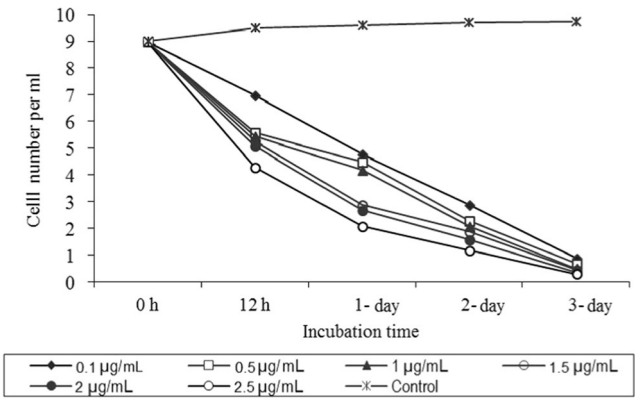

Fig. 7 Growth of *E. coli* ATCC11229 in low concentrations of SNPs

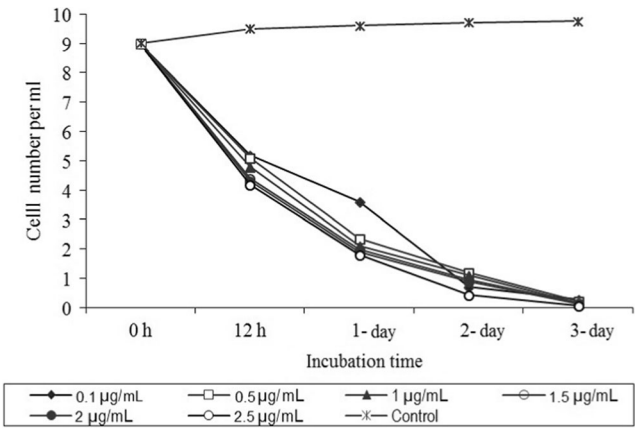

Fig. 8 Growth of *S. aureus* ATCC6538 in low concentrations of SNPs

(2013b) reported that increasing initial concentrations of pullulan and silver nitrate resulted in a substantial increase in the SPR bands, and maximum absorption peak was observed by adding 12 mol/L of silver nitrate. Similar results were obtained in our research, when 10 mol/L $AgNO_3$ was applied. In this concentration, synthesized SNPs gave a broad band at 420 nm (Fig. 1b).

In our experiments, nanoparticles size varied from 5 to 50 nm, when TEM micrographs were taken from overall samples of SNPs. But SNPs, synthesized with HMW EPS (absorption maximum at 450 nm), formed a big size particles (20–50 nm), whereas on the matrix of LMW, EPS formed relatively small (about 5–20 nm) SNPs with absorption maximum at 420 nm. Dang et al. (2011) explained the formation of different size nanoparticles with a collision between them, which leads to nanoparticles' growth. We think that it might be also due to chemical structures of polysaccharide chain and physical properties of SNPs containing solutions. As concluded by Hamedi et al. (2012), utilization of starch and β-D-glucose in the synthesis of SNPs resulted in the formation of smaller particles to those obtained with help of extracts of microbial cultures. Average size of particles, synthesized with polysaccharides, varied between 20 and 30 nm, whereas in other studies, the size and shape differed. Kanmani and Lim (2013b) report pullulan-mediated SNPs with sizes of 2–40 nm, Bankura et al. (2012) with 5–10-nm-sized particles, after stabilization the silver ions with dextran. Furthermore, Yen et al. (2009) investigated SNPs with 3–25 nm size, whereas Abdel-Mohsen et al. (2014)–6 nm and Haiza et al. (2013)–15.63 to 26.05-nm-sized SNPs.

XRD analysis confirmed the presence of atomic Ag at 47.5, 55.5, and 64.5 in the 2 theta region. Comparison of the XRD spectra of both types of SNPs, synthesized with the help of LMW and HMW EPS, showed that peaks' position was similar in all samples. It can be explained, as documented above, by the presence of the same monomeric units in both LMW and HMW EPS of *B. japonicum*. Besides, FTIR also gave substantial evidence that silver nanoparticle influenced the stretching in the IR spectra. An analogical data was documented by Kanmani and Lim (2013a) at 1384/cm with pullulan-stabilized SNPs (Kanmani and Lim 2013a). The presence of peak at 1236/cm discriminates the bacterial polysaccharides from other polysaccharides (Kanmani and Lim 2013a, b). These observations suggest a strong interaction of Ag with the EPS (Fig. 4).

We investigated dose-dependent inhibition of the tested strains, *E. coli* ATCC11229 and *S. aureus* ATCC6538, in both agar media and broth. Dose-dependent antimicrobial effects of SNPs are reported for pathogens such as *E. coli*, *Bacillus cereus*, *Streptococcus pyogenes* (Yoksan and Chirachanchai 2010; Priyadarshini et al. 2013), *Pseudomonas aeruginosa* (Hebeish et al. 2013; Kora and Arunachalam 2011), *Bacillus subtilis* (Wei et al. 2012), *Salmonella typhus* (Morones et al. 2005), *S. aureus*, *Mycobacterium tuberculosis* (Hebeish et al. 2013; Song et al. 2006), *Klebsiella pneumoniae*, *Listeria monocytogenes* (Kanmani and Lim 2013a, b). The Gram-negative bacterial pathogens were highly suppressed by the SNPs compared to Gram-positive bacterial pathogens (Kanmani and Lim 2013a). This explains that the Gram-positive bacteria are composed of a three-dimensional thick peptidoglycan (~20–80 nm) layer compared to that of Gram-negative bacteria (~7–8 nm). The peptidoglycan layer possessing linear polysaccharide chains is cross-linked by more short peptides and thus forms complex structure leading to difficult penetration of SNPs into the Gram-positive bacteria compared to that of Gram-negative bacteria (Priyadarshini et al. 2013).

Some authors reported treatment with low concentrations of SNPs. Kora and Arunachalam (2011) report 4 μg/mL SNPs against *P. aeruginosa* and Wei et al. (2012) 9 μg/mL SNPs against *B. subtilis* and *E. coli*. Increasing the SNPs' concentration resulted in high inhibition zones. For instance, Bankura et al. (2012) reported that in 200 μg/mL concentration of SNPs, the inhibition zone diameters of *E. coli*, *P. aeruginosa*, *B. cereus*, and *B. subtilis* were 21, 24, 28, and 32 mm, respectively. Analogical results were obtained in our researches, when the SNP concentrations ranged from 0.25 to 2.5 μg/mL. Depending on the SNP (synthesized on the LMW EPS) concentrations, the inhibition zones of the pathogens differed from 16 to 32 mm, and maximal activity was observed with 2.5 μg/mL SNP (Figs. 5 and 6). When HMW EPS-stabilized SNPs were applied, the inhibition zones varied between 6 and 22 mm, respectively. We explain the difference in antibacterial activity with solubility of SNPs applied. The higher the solubility of the SNPs, the higher activity was observed in our experiments.

In all treated with SNP cases, a substantial decrease in relative cell viability was observed. But it is necessary to point out that SNPs' antibacterial activity depended on chemical structure and physical properties of matrix used for silver reduction and stabilization. SNPs, synthesized on the matrix of LMW EPS, highly suppressed cell -population than that of

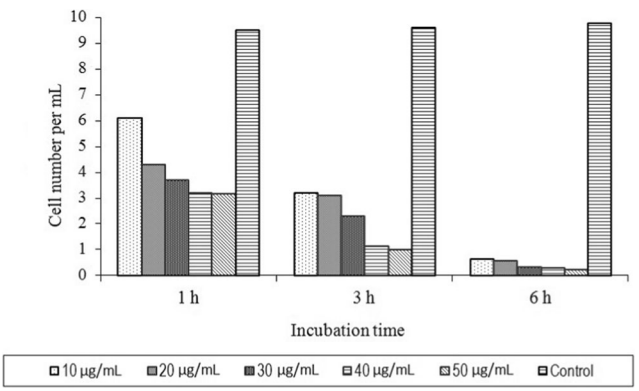

Fig. 9 Influence of SNPs on the cell viability of *E. coli* ATCC11229 in high concentrations of SNPs

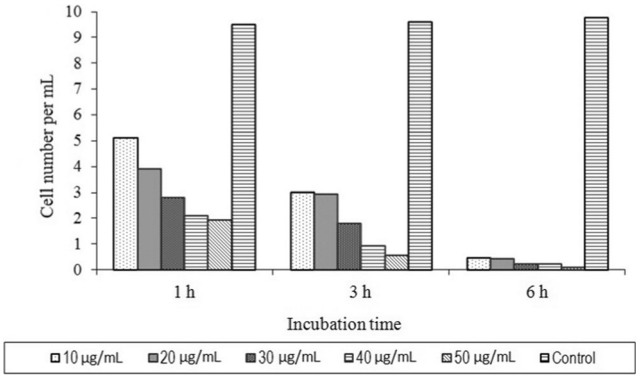

Fig. 10 Influence of SNPs on the cell viability of *S. aureus* ATCC6538 in high concentrations of SNPs

synthesized on the matrix of HMW EPS. The results of kill-curve experiments showed that the pathogens were sensitive even to relatively low concentrations of SNPs, synthesized via reducing with LMW EPS; but in low concentrations, the efficiency of SNPs was noticeable within 3 days of incubation. In some concentrations, after the second and third days of incubation, a substantial part of bacterial cells formed dead biomass in the bottom of the test tubes, turning the thick liquid into transparent liquid. The most effective concentration of SNPs was 30 μg/mL. In higher concentrations of SNPs (>30 μg/mL), the results were the same as in the case of 30 μg/mL (Figs. 9 and 10). After 6 h of incubation with 30, 40, and 50 μg/mL SNPs, more than 95 % of the bacterial cell population was killed.

When SNPs were applied, synthesized on the matrix of HMW EPS, the antibacterial activity was lower than that of synthesized on the matrix of LMW EPS.

Similar results were reported by many authors with different concentrations of SNPs. Kanmani and Lim (2013b) reported that more than 50 and 70 % of cells of *P. aeruginosa* were dead after 2 h long incubation with 70 and 100 μg/mL SNPs, respectively. After 6 h no cell viability was observed. According to Mohanty et al. (2012), 98 % of the cell population of *S. aureus*, *P. aeruginosa*, *Shigella flexneri*, and *Salmonella typhi* was killed at 2 μM of SNPs after 4 h, whereas Shukla et al. (2012) documented a significant reduction in the cell viability of *Bacillus pumilus* in the presence of 500 μM SNPs (Shukla et al. 2012).

In conclusion, LMW and HMW EPS of the diazotrophic strain *B. japonicum* 36 can reduce Ag^{+} from $AgNO_3$ and synthesize SNPs with separate absorption maximums at 420 and 450 nm. Interesting to note that the nanoparticles' size and shape differed in these samples, ranged between 5 and 50 nm. Besides, SNPs, synthesized on the matrix of LMW EPS, successfully demonstrated itself as an antimicrobial agent against some pathogens, compared with HMW EPS, such as *E. coli*, *S. aureus*, and *C. albicans*. LMW EPS of *B. japonicum* 36 was recommended for synthesis and application of SNPs with high antimicrobial activity. After treatment with high concentrations of SNPs (LMW EPS), the relative cell viability began to drop after 2 h of incubation. The most effective concentration of SNPs was 30 μg/mL. The above-discussed kill-curve experiments confirmed the strong antibacterial properties of SNPs, synthesized on the matrix of LMW EPS, both in a powder and colloidal forms.

Acknowledgments This work was supported by the Projects of International Cooperation and Exchanges of the National Natural Science Foundation of China (Grant No. 31110103908), the Projects of International Science & Technology Cooperation of the Xinjiang Uyghur Autonomous Region (Grant No. 20126023), and the Central Asian Drug Discovery and Development Center of Chinese Academy of Sciences.

Compliance with ethical standards

Conflict of interest The authors declare that they have no conflict of interest.

References

Abdel-Mohsen AM, Abdel-Rahman RM, Moustafa MGF, Vojtova L, Uhrova L, Hassan AF, Al-Deyab SS, El-Shamy IE, Jancar J (2014) Preparation, characterization and cytotoxicity of schizophyllan/silvernanoparticle composite. Carbohydr Polym 102:238–245

Aslan K, Lakowicz JR, Geddes CD (2005) Fast and slow deposition of silver nanorods on planar surfaces: application to metal-enhanced fluorescence. J Phys Chem B 109(8):3157–3162

Bankura KP, Maity D, Mollick MMR, Mondal D, Bhowmick B, Bain MK (2012) Synthesis, characterization and antimicrobial activity of dextran stabilized silver nanoparticles in aqueous medium. Carbohydr Polym 89:1159–1165

Battisti L, Lara JC, Leigh JA (1992) Specific oligosaccharide form of the *Rhizobium meliloti* exopolysaccharide promotes nodule invasion in alfalfa. Proc Natl Acad Sci U S A 89:5625–5629

De Cremer G, Sels BF, Hotta J-I, Roeffaers MBJ, Bartholomeeusen E, Coutino-Gonzales E, Valtchev V, De Vos DE, Vosh T, Hofkens J (2010) Optical encoding of silver zeolite microcarriers. Adv Mater 22(9):957–960

Dang TMD, Le TTT, Fribourg-Blanc E, Dang MC (2011) Synthesis and optical properties of copper nanoparticles prepared by a chemical reduction method. Adv Nat Sci: Nanosci Nanotechnol 2, 015009 **(6 pp)**

Dubois M, Gilles KA, Hamilton JK, Rebers PA, Smith F (1956) Colorimetric method for determination of sugars and related substances. Anal Chem 28(3):350–356

Feng QL, Wu J, Chen GQ, Cui FZ, Kim TN, Kim JO (2000) A mechanistic study of the antibacterial effect of silver ions on *E. coli* and *Staphylococcus aureus*. J Biomed Mater Res 52:662–668

Filippo E, Serra A, Buccolieri A, Manno D (2010) Green synthesis of silver nanoparticles with sucrose and maltose: morphological and structural characterization. J Non-Cryst Solids 356:344–350

Gajbhiye M, Kesharwani J, Ingle A, Gade A, Rai M (2009) Fungus-mediated synthesis of silver nanoparticles and their activity against pathogenic fungi in combination with fluconazole. Nanomed: Nanotechnol Biol Med 5:382–386

Haiza H, Aziza A, Mohidin AH, Halin DSC (2013) Green synthesis of silver nanoparticles using local honey. Nano Hybrids 4:87–98

Hamedi S, Ghaseminezhad SM, Shojaosadati SA, Shokrollahzadeh S (2012) Comparative study on silver nanoparticles properties produced by green methods. Iran J Biotechnol 10(3):191–197

Hebeish A, Hashem M, Abd El-Hady MM, Sharaf S (2013) Development of CMC hydrogels loaded with silver nanoparticles for medical applications. Carbohydr Polym 92:407–413

Jain N, Bhargava A, Majumdar S, Tarafdar GC, Panwar J (2011) Extracellular biosynthesis and characterization of silver nanoparticles using *Aspergillus flavus* NJP08: a mechanism perspective. Nanoscale 3:635

Kalimuthu K, Babu RS, Venkataraman D, Bilal M, Gurunathan (2008) Biosynthesis of silver nanoparticles by *Bacillus licheniformis*. Colloids Surf B 65:150–153

Kanmani P, Lim ST (2013a) Synthesis and structural characterization of silver nanoparticles using bacterial exopolysaccharide and its antimicrobial activity against food and multidrug resistant pathogens. Process Biochem 48:1099–1106

Kanmani P, Lim ST (2013b) Synthesis and characterization of pullulan-mediated silver nanoparticles and its antimicrobial activities. Carbohydr Polym 97:421–428

Kanmani P, Satish KR, Yuvaraj N, Paari KA, Pattukumar V, Arul V (2012) Probiotics and its functionally valuable products. Crit Rev Food Sci Nutr 53:641–658

Kim SH, Hyeong SL, Deok SR, Soo JC, Lee DS (2011) Antibacterial activity of silver-nanoparticles against *Staphylococcus aureus* and *Escherichia coli*. Korean J Microbiol Biotechnol 39(1):77–85

Kora AJ, Arunachalam J (2011) Assessment of antibacterial activity of silver nanoparticles on *Pseudomonas aeruginosa* and its mechanism of action. World J Microbiol Biotechnol 27:1209–1216

Lara HH, Ayala-Nunez NV, Ixtepan-Turrent L, Rodriguez-Padilla C (2010) Mode of antiviral action of silver nanoparticles against HIV-1. J Nanobiotechnology 8(1):31–39

Li J, Tian X, Habasi M, Chen K, Pang N, Hu P, Aisa HA (2012) A phytoreduction route for selective synthesis of highly stable Ag and Ag:AgCl hybrid nanocolloids. Cryst Eng Comm 14:7621–7625

Louch H, Miller KJ (2001) Synthesis of a low-molar-mass form of exopolysaccharide by *Bradyrhizobium japonicum* USDA 110. Appl Environ Microbiol 67(2):1011–1014

Mohanty S, Mishra S, Jena P, Jacob B, Sarkar B, Sonawane A (2012) An investigation on the antibacterial, cytotoxic, and antibiofilm efficacy of starch-stabilized silver nanoparticles. Nanomed: Nanotechnol Biol Med 8:916–924

Morones JR, Elechiguerra JL, Camacho A, Holt K, Kouri JB, Ramirez JT (2005) The bactericidal effect of silver nanoparticles. Nanotechnology 16:2346–2353

Nanda A, Saravanan M (2009) Biosynthesis of silver nanoparticles from *Staphylococcus aureus* and its antimicrobial activity against MRSA and MRSE. Nanomed: Nanotechnol Biol Med 5:452–456

Panacek A, Kolar M, Vecerova R, Prucek R, Soukupova J, Krystof VL (2009) Antifungal activity of silver nanoparticles against *Candida* spp. Biomaterials 30:6333–6340

Pandey S, Goswami GK, Nanda KK (2012) Green synthesis of biopolymer–silver nanoparticle nanocomposite: an optical sensor for ammonia detection. Int J Biol Macromol 51:583–589

Priyadarshini S, Gopinath V, Meera PN, Mubarak AD, Velusamy P (2013) Synthesis of anisotropic silver nanoparticles using novel strain, *Bacillus flexus* and its biomedical application. Colloids Surf B 102:232–237

Quelas JI, Lopez-Garcia SL, Casabuono A, Althabegoiti MJ, Mongiardini EJ, Perez-Gimenez J, Couto A, Lodeiro AR (2006) Effects of N-starvation and C-source on *Bradyrhizobium japonicum* exopolysaccharide production and composition and bacterial infectivity to soybean roots. Arch Microbiol 186:119–128

Rasulov BA (2014) Obtaining and activity of silver nanoparticles based on the exopolysaccharide of diazotrophic strain *Bradyrhizobium japonicum* 36 and $AgNO_3$. Biotechnologia Acta 7:57–62

Rasulov BA, Yili A, Aisa HA (2013) Biosorption of metal ions by exopolysaccharide produced by *Azotobacter chroococcum* XU1. J Environ Prot 4:989–993

Santander-Ortega MJ, de la Fuente M, Lozano MV, Bekheet ME, Progatzky F, Elouzi A (2012) Hydration forces as a tool for the optimization of core–shell nanoparticle vectors for cancer gene therapy. Soft Matter 8:12080–12092

Sastry M, Mayya KS, Patil V, Paranjape DV, Hegde SG (1997) Langmuir-Blodgett films of carboxylic acid derivatized silver colloidal particles: role of subphase pH on degree of cluster incorporation. J Phys Chem B 101:4954–4958

Shafer-Peltier KE, Haynes CL, Glucksberg MR, Van Duyne RP (2003) Toward a glucose biosensor based on surface-enhanced Raman scattering. J Am Chem Soc 125:588

Shukla MK, Singh RP, Reddy CRK, Jha B (2012) Synthesis and characterization of agar-based silver nanoparticles and nanocomposite film with antibacterial applications. Bioresour Technol 107:295–300

Song HY, Ko KK, Lee BT (2006) Fabrication of silver nanoparticles and their antimicrobial mechanisms. Eur Cell Mater 11:58–59

Vigneshwaran N, Nachane RP, Balasubramanya RH, Varadarajan PV (2006) A novel one-pot 'green' synthesis of stable silver nanoparticles using soluble starch. Carbohydr Res 341:2012–2018

Wei X, Luo M, Li W, Yang L, Liang X, Xu L (2012) Synthesis of silver nanoparticles by solar irradiation of cell-free *Bacillus amyloliquefaciens* extracts and $AgNO_3$. Bioresour Technol 103: 273–278

Yen HJ, Hsu SH, Tsai CL (2009) Cytotoxicity and immunological response of gold and silver nanoparticles of different sizes. Small 5: 1553–1561

Yoksan R, Chirachanchai S (2010) Silver nanoparticle-loaded chitosan–starch based films: fabrication and evaluation of tensile, barrier and antimicrobial properties. Mater Sci Eng C 30:891–897